Electronic Supplementary Material (ESI) for CrystEngComm
This journal is © The Royal Society of Chemistry 2012

Supporting Information

Chemistry of density: extension and structural origin of Carnelley's rule in chloroethanes

Marcin Podsiadło,[a] Maciej Bujak[b] and Andrzej Katrusiak[a]

[a]Faculty of Chemistry, Adam Mickiewicz University, Grunwaldzka 6, 60-780 Poznań, Poland. E-mail: katran@amu.edu.pl; Fax: +48(61)829-1505; Tel: +48(61)829-1443; [b]Faculty of Chemistry, University of Opole, Oleska 48, 45-052 Opole, Poland. E-mail: mbujak@uni.opole.pl; Fax: +48(77)452-7101; Tel:+48(77)452-7100

Experimental

High-pressure study

Chloroethane, C_2H_5Cl, MCE, for synthesis (m.p. 134 K, b.p. 285 K, ≥99%, Merck) was loaded to a modified Merrill-Bassett (Bassett, W. A. (2009). *High Press. Res.* **29**, 163-186) diamond-anvil cell (DAC) at cryogenic conditions and *in situ* crystallized. The gasket, made of 0.3 mm thick tungsten foil with spark-eroded 0.4 mm hole, was pre-indented to *ca.* 0.25 mm. At 295 K chloroethane froze at 2.6 GPa in the form of polycrystalline mass filling all volume of the high-pressure chamber. Pressure was calibrated by the ruby fluorescence method (Piermarini, G. J., Block, S., Barnett, J. D. & Forman, R. A. (1975). *J. Appl. Phys*. **46**, 2774-2780) using a BETSA PRL spectrometer with the accuracy of 0.05 GPa, before and after the X-ray diffraction measurements.

The single-crystal of chloroethane was obtained in isochoric conditions: the DAC with the polycrystalline mass was heated using a hot-air gun to *ca.* 400 K when all but one grain melted. This single crystal grew as the DAC was cooled slowly and eventually filled the whole volume of the chamber. The final pressure stabilized at 2.62 GPa. The gasket was 0.15 mm thick and the spark-eroded hole had the diameter of 0.31 mm (these were the dimensions of the single crystal). The progress in growing the single crystal is shown in Figure S1. After collecting the diffraction data (Budzianowski, A. & Katrusiak, A. (2004). *High-Pressure Crystallography*, edited by A. Katrusiak & P.F. McMillan, pp. 101-112. Dordrecht: Kluwer Academic Publishers), the pressure was increased and the DAC was heated again to *ca.* 460 K, till the single crystal occupied about 10 % of the chamber volume. Then the crystal was grown again by controlled cooling to room temperature and 3.04(5) GPa. The single crystal filled completely the DAC chamber (Figure S2), and it was used for the next X-ray diffraction measurement (Budzianowski, A. & Katrusiak, A. (2004). *High-Pressure Crystallography*, edited by A. Katrusiak & P.F. McMillan, pp. 101-112. Dordrecht: Kluwer Academic Publishers).

This journal is © The Royal Society of Chemistry 2012

The single-crystal reflection data were collected at 295 K using a KM-4 CCD diffractometer with the graphite-monochromated MoK_α radiation. The DAC was centred by the gasket-shadow method (Budzianowski, A. & Katrusiak, A. (2004). *High-Pressure Crystallography*, edited by A. Katrusiak & P.F. McMillan, pp. 101-112. Dordrecht: Kluwer Academic Publishers). The reflections were collected with the ω- and φ-scan frames of 0.75º and the exposure time of 45 s (Budzianowski, A. & Katrusiak, A. (2004). *High-Pressure Crystallography*, edited by A. Katrusiak & P.F. McMillan, pp. 101-112. Dordrecht: Kluwer Academic Publishers). The *CrysAlisCCD* and *CrysAlisRED* programs (Oxford Diffraction (2007). *CrysAlis CCD* and *CrysAlis RED*. Versions 1.171.32. Oxford Diffraction, Abingdon, Oxfordshire, England) were used for the data collection, determination of the *UB*-matrix, and for initial data reduction and *Lp* corrections. The reflections intensities have been accounted for the effect of absorption of X-rays by the DAC, shadowing of the beams by the gasket edges and absorption of the sample crystal itself (Katrusiak, A. (2003). *REDSHABS*. Program for correcting reflections intensities for DAC absorption, gasket shadowing and sample crystal absorption. Adam Mickiewicz University, Poznań, Poland.; Katrusiak, A. (2004). *Z. Kristallogr*. **219**, 461-467). The structure was solved by direct methods using program *SHELXS-97* (Sheldrick, G. M. (2008). *Acta Cryst.* A**64**, 112-122), and refined with anisotropic displacement parameters for non-H atoms by program *SHELXL-97* (Sheldrick, G. M. (2008). *Acta Cryst.* A**64**, 112-122). The H-atoms were located in the Fourier-difference maps and freely refined (Sheldrick, G. M. (2008). *Acta Cryst.* A**64**, 112-122).

Low-temperature study

Chloroethane was inserted in the form of a 0.3 mm long drop into a 0.3 mm in diameter glass capillary and mounted on a four-circle KUMA KM-4 CCD diffractometer with the graphite-monochromated MoK_α radiation. The temperature was controlled by an Oxford Diffraction Cryosystems CPC611 attachment. The sample froze into a single crystal when rapidly cooled to 120 K (14 K below the m.p. of MCE), and its diffraction data were collected. Than the crystal was cooled down (1 $K \cdot min^{-1}$) and the next diffraction measurement was performed at 100 K. At 120 and 100 K the reflections were measured using the ω-scan technique with $\Delta\omega$ = 1.0 º and 1.5 s exposure time. The data were accounted for the Lorentz polarization and sample absorption effects (Oxford Diffraction (2007). *CrysAlis CCD* and *CrysAlis RED* versions 1.171.32. Oxford Diffraction, Abingdon, Oxfordshire, England.; Sheldrick, G. M. (2008). *Acta Cryst.* A**64**, 112-122). The structure was solved by direct methods using program *SHELXS-97* (Sheldrick, G. M. (2008). *Acta Cryst.* A**64**, 112-122), and refined with

This journal is © The Royal Society of Chemistry 2012

anisotropic displacement parameters for non-H atoms by program *SHELXL-97* (Sheldrick, G. M. (2008). *Acta Cryst.* A**64**, 112-122). The H-atoms were located in the difference-Fourier maps and refined freely with an isotropic displacement parameter (Sheldrick, G. M. (2008). *Acta Cryst.* A**64**, 112-122). Selected details of the MCE phase I and II structure refinements and crystal data are listed in Table S1.

Program *CrystalExplorer* (Grimwood, D. J., Jayatilaka, D., McKinnon, J. J., Spackman, M. A. & Wolff, S. K. *CrystalExplorer*, University of Western Australia, Crowley, ver. 2.1, 2008) and a PC were used for calculations of the electrostatic potential on the molecular surfaces of MCE. Electrostatic potential (Murray, J. N. & Sen, K. D. (1996). *Molecular Electrostatic Potential: Concepts and Applications*; Elsevier: New York) was mapped onto the molecular surfaces defined as 0.001 a.u. electron-density envelope (Bader, R. F. W., Carroll, M. T., Cheeseman, J. R. & Chang, C. (1987). *J. Am. Chem. Soc.* **109**, 7968-7979).

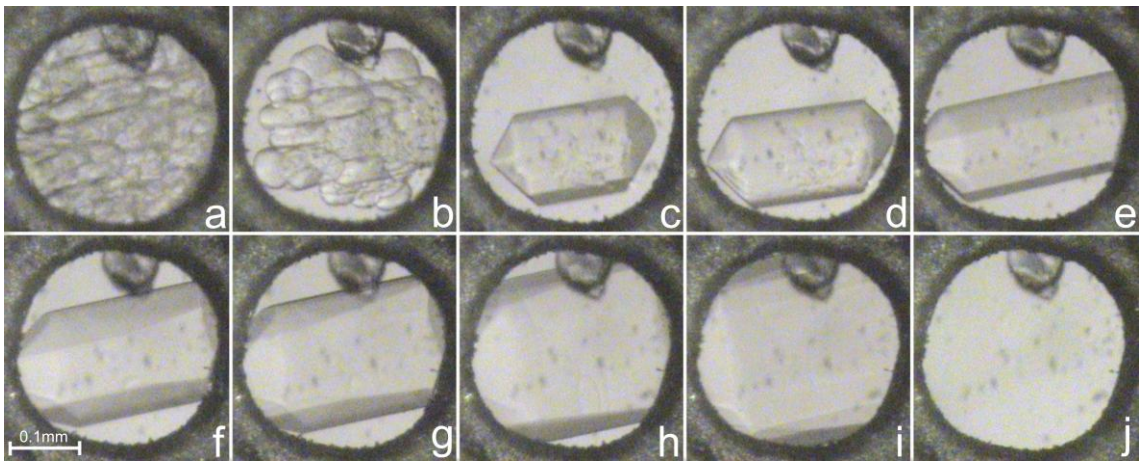

Figure S1. Stages of the isochoric single-crystal growth of chloroethane inside the DAC chamber: (a) polycrystalline mass at 380 K; (b) polycrystalline mass at 400 K; (c) a single-crystal seed at 390 K; (d-i) the single-crystal cooled to 360 K; (j) the DAC chamber completely filled by the single-crystal at 295 K and 2.62 GPa. The small ruby chip for pressure calibration lies at the upper edge of the gasket.

This journal is © The Royal Society of Chemistry 2012

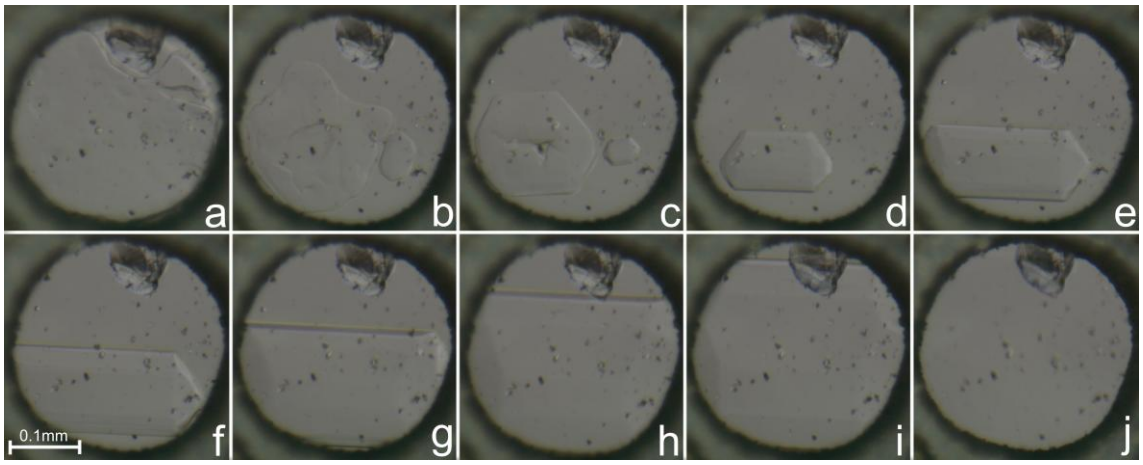

Figure S2. Stages of isochoric C_2H_5Cl single-crystal growth inside the DAC chamber viewed in transmission-light mode: (a) at 440 K; (b, c) two crystal seeds at 450 K; (d) one crystal seed at 460 K; (e-i) the growing crystal on lowering temperature; (j) the single-crystal filling whole volume of the DAC chamber at 3.04 GPa/295 K. The ruby chip is located as in Figure S1.

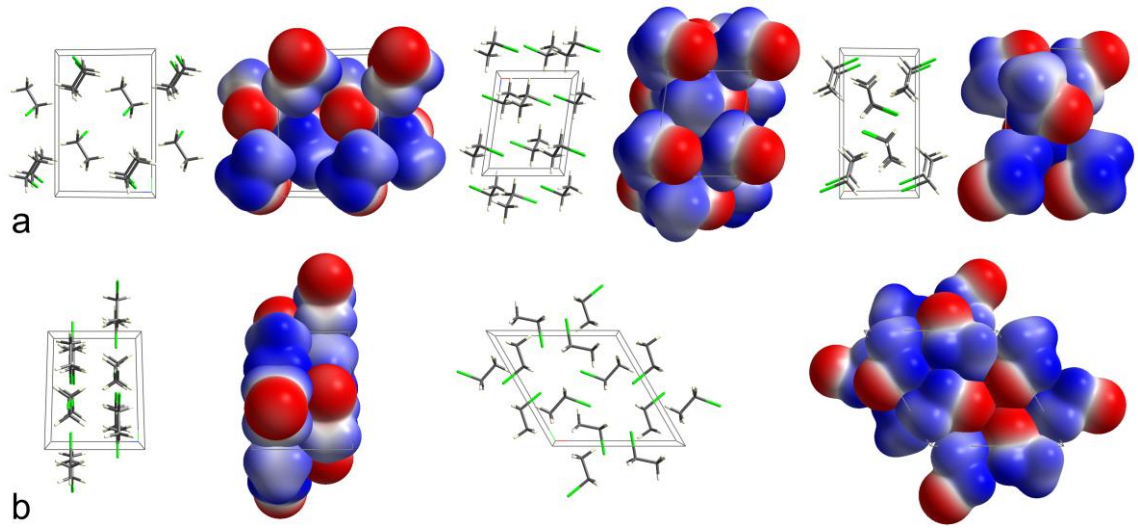

Figure S3. The characteristic patterns of interacting molecules observed in the structures of MCE phase I (a) viewed along ***a***, ***b*** and ***c***, and phase II (b) viewed along ***a*** and ***c***. Electrostatic potential (Murray, J. N. & Sen, K. D. (1996). *Molecular Electrostatic Potential: Concepts and Applications*; Elsevier: New York) was mapped onto the molecular surfaces defined as 0.001 a.u. electron-density envelope (Bader, R. F. W., Carroll, M. T., Cheeseman, J. R. & Chang, C. (1987). *J. Am. Chem. Soc.* **109**, 7968-7979); the electrostatic potential scale ranging from -0.038 a.u. (-88.11 kJ/mol; red) to 0.03 a.u. (89.77 kJ/mol; blue) is common for all these drawings.

This journal is © The Royal Society of Chemistry 2012

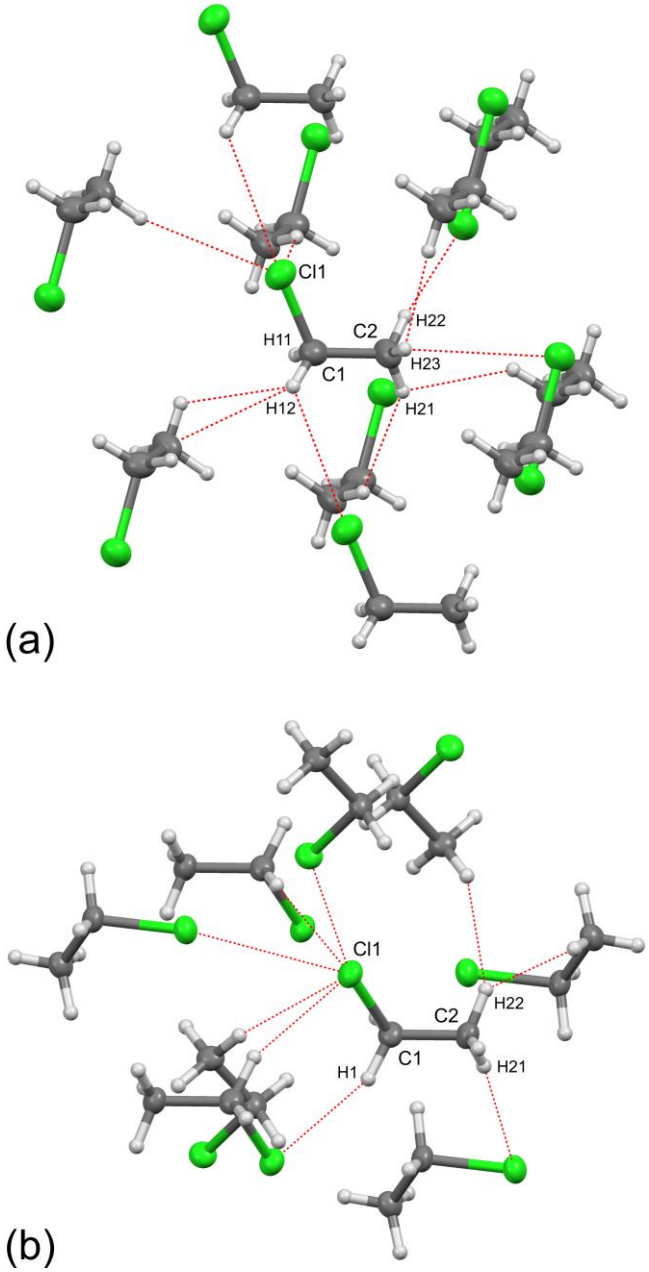

Figure S4. The shortest intermolecular Cl···Cl, H···Cl and H···H distances, denoted by the red dashed lines, made by the single MCE molecule at (a) 0.1 MPa/100 K and (b) 3.04 GPa/295 K (Table S3). Displacement ellipsoids are plotted at the 50% probability level.

This journal is © The Royal Society of Chemistry 2012

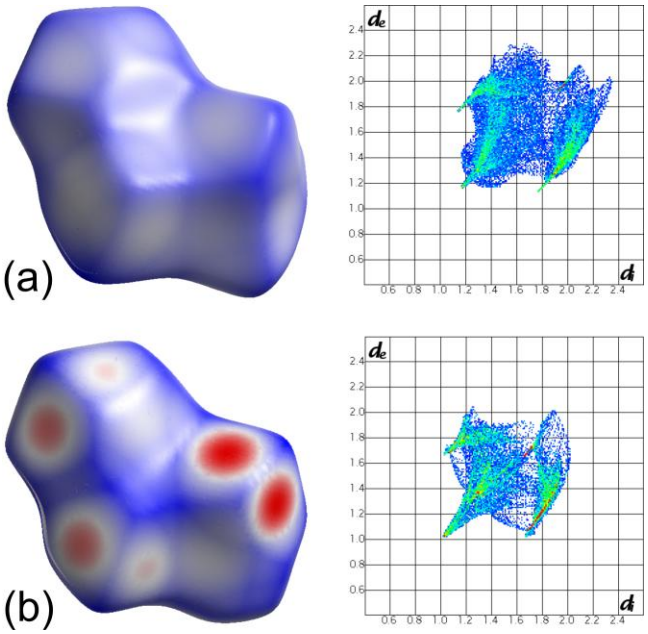

Figure S5. The Hirshfeld surfaces (Grimwood, D. J., Jayatilaka, D., McKinnon, J. J., Spackman, M. A. & Wolff, S. K. *CrystalExplorer*, University of Western Australia, Crowley, ver. 2.1, 2008) together with the corresponding two-dimensional fingerprint plots for the MCE molecule at (a) 0.1 MPa/100 K and (b) 3.04 GPa/295 K. The colour scale describes distances longer (navy-blue), equal (white), and shorter (red) than the sum of van der Waals radii.

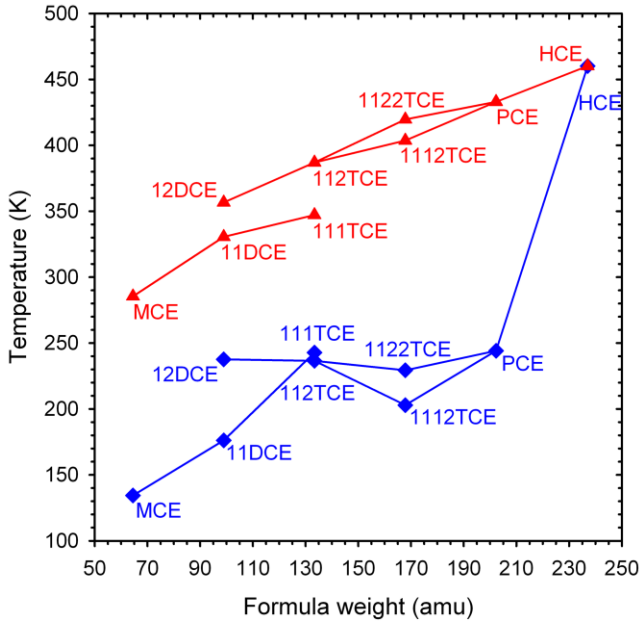

Figure S6. The ambient-pressure melting (blue diamonds) and boiling (red triangles) points of chloroethanes in the function of their formula weight (Lide, D. R. (1994). CRC Handbook of Chemistry and Physics, 75th ed., CRC Press Inc., Boca Raton, FL). MCE – chloroethane;

This journal is © The Royal Society of Chemistry 2012

11-, 12DCE – 1,1-, 1,2-dichloroethane; 111-, 112TCE – 1,1,1-, 1,1,2-trichloroethane; 1112-, 1122TCE – 1,1,1,2-, 1,1,2,2-tetrachloroethane; PCE – pentachloroethane; HCE – hexachloroethane.

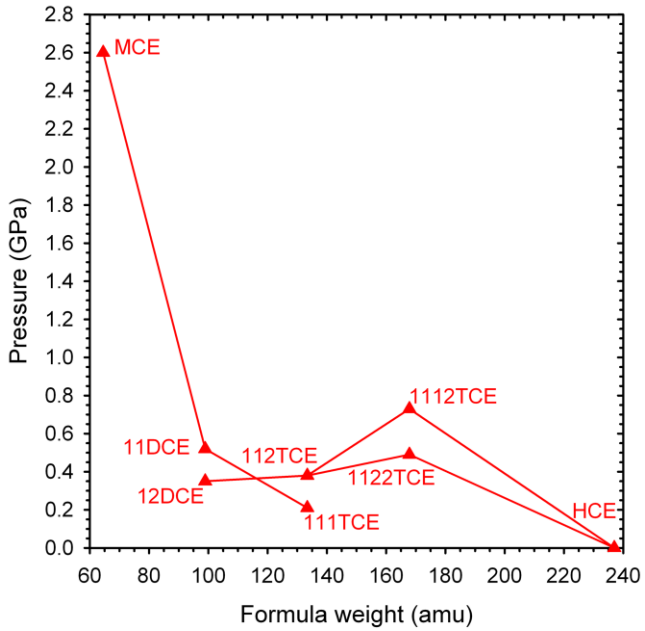

Figure S7. The room-temperature freezing point in the function of formula weight for: chloroethane, MCE (this work); 1,1-dichloroethane, 11DCE (Bujak, M., Podsiadło, M. & Katrusiak, A. (2008). *J. Phys. Chem. B* **112**, 1184-1188); 1,2-dichloroethane, 12DCE (Bujak, M., Podsiadło, M. & Katrusiak, A., in preparation); 1,1,1-trichloroethane, 111TCE (Bujak, M., Podsiadło, M. & Katrusiak, A. (2011). *CrystEngComm*. **13**, 396-398); 1,1,2-trichloroethane, 112TCE (Bujak, M., Podsiadło, M. & Katrusiak, A. (2008). *Chem. Commun.* 4439-4441); 1,1,1,2-tetrachloroethane, 1112TCE (Bujak, M. & Katrusiak, A. (2010). *CrystEngComm*. **12**, 1263-1268); 1,1,2,2-tetrachloroethane, 1122TCE (Bujak, M., Bläser, D., Katrusiak, A. & Boese, R. (2011). *Chem. Commun.* **47**, 8769-8771) and hexachloroethane, HCE.

This journal is © The Royal Society of Chemistry 2012

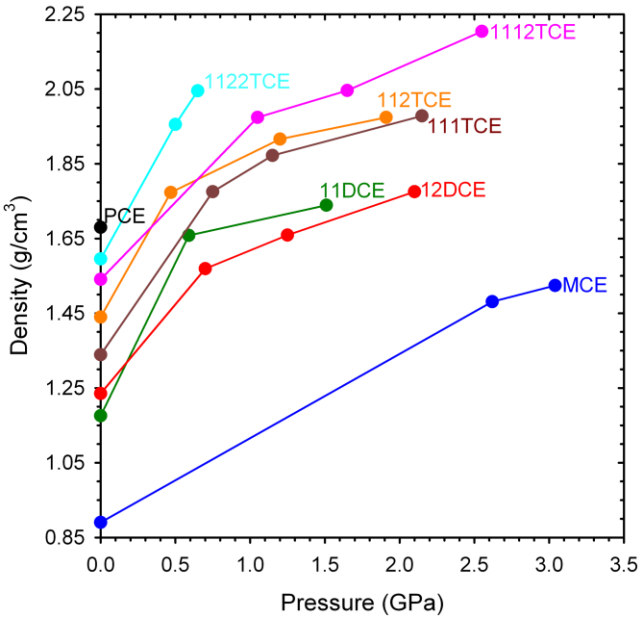

Figure S8. The density of liquid, at ambient conditions, chloroethanes in the function of pressure at 293 K (298 K for chloroethane) (Lide, D. R. (1994). CRC Handbook of Chemistry and Physics, 75th ed., CRC Press Inc., Boca Raton, FL) and in the solid state, at room temperature, for: chloroethane (blue) (this work); 1,1-dichloroethane (green) (Bujak, M., Podsiadło, M. & Katrusiak, A. (2008). *J. Phys. Chem. B* **112**, 1184-1188); 1,2-dichloroethane (red) (Bujak, M., Budzianowski, A. & Katrusiak, A. (2004). *Z. Kristallogr.* **219**, 573-579; Bujak, M., Podsiadło, M. & Katrusiak, A., in preparation); 1,1,1-trichloroethane (brown) (Bujak, M., Podsiadło, M. & Katrusiak, A. (2011). *CrystEngComm*. **13**, 396-398); 1,1,2-trichloroethane (orange) (Bujak, M., Podsiadło, M. & Katrusiak, A. (2008). *Chem. Commun.* 4439-4441); 1,1,1,2-tetrachloroethane (pink) (Bujak, M. & Katrusiak, A. (2010). *CrystEngComm*. **12**, 1263-1268); 1,1,2,2-tetrachloroethane, (cyjan) (Bujak, M. & Katrusiak, A. (2004). *Z. Kristallogr.* **219**, 669-674; Bujak, M., Bläser, D., Katrusiak, A. & Boese, R. (2011). *Chem. Commun.* **47**, 8769-8771). The black dot is for the density of liquid pentachloroethane.

This journal is © The Royal Society of Chemistry 2012

Table S1. Crystal data and details of the refinements of MCE phase I at 120 and 100 K (all at 0.1 MPa) and phase II at 2.62 and 3.04 GPa (all at 295 K).

	C_2H_5Cl phase I	C_2H_5Cl phase I	C_2H_5Cl phase II	C_2H_5Cl phase II
Pressure (GPa)	10^{-4}	10^{-4}	2.62(5)	3.04(5)
Temperature (K)	120.0(1)	100.0(1)	295(2)	295(2)
Formula weight	64.51	64.51	64.51	64.51
Crystal colour	colourless	colourless	colourless	colourless
Crystal size (mm)	0.2 x 0.2 x 0.2	0.2 x 0.2 x 0.2	0.32 x 0.31 x 0.15	0.31 x 0.30 x 0.14
Crystal system	monoclinic	monoclinic	hexagonal	hexagonal
Space group	$P2_1/n$	$P2_1/n$	$P6_3/m$	$P6_3/m$
Unit cell dimensions (Å; °) a =	5.3006(7)	5.2815(6)	8.8941(13)	8.8116(12)
b =	9.8562(15)	9.8152(14)	8.8941(13)	8.8116(12)
c =	6.8405(10)	6.7653(9)	6.3353(13)	6.2705(13)
β =	98.173(13)	98.071(12)	90	90
Volume (Å^3)	353.74(9)	347.23(8)	434.01(13)	421.64(12)
Z	4	4	6	6
D_x (g cm^{-3})	1.211	1.234	1.481	1.524
Wavelength MoKα, λ (Å)	0.71073	0.71073	0.71073	0.71073
Absorption coefficient (mm^{-1})	0.80	0.81	0.97	1.00
F(000) (e)	136	136	204	204
2θ max (°)	49.98	49.98	55.74	54.22
Min./Max. indices h,k,l	-6/6, -11/11, -8/8	-6/6, -11/11, -8/7	-11/11, -5/5, -8/8	-11/10, -4/4, -8/8
Reflections collected/unique	2120/620	2344/609	1918/196	1640/169
R_{int}	0.0655	0.0726	0.0329	0.0357
Observed reflections (I>2σ(I))	521	518	191	167
Data/parameters	620/48	609/48	196/30	169/30
Goodness of fit on F^2	1.072	0.999	1.182	1.096
Final R_1 indices (I>2σ(I))	0.0600	0.0552	0.0215	0.0172
R_1/wR_2 indices (all data)	0.0654/0.1540	0.0602/0.1433	0.0226/0.0515	0.0175/0.0442
Completeness (%)	100	100	52	50
$\Delta\sigma_{max}$, $\Delta\sigma_{min}$ (eÅ^{-3})	0.78, -0.31	0.68, -0.34	0.25, -0.15	0.14, -0.11
Weighting scheme: x; y[a]	0.1140; 0	0.1180; 0	0.0209; 0.17	0.0204; 0.12
Absorption corrections	capillary and sample crystal	capillary and sample crystal	DAC, gasket and sample crystal	DAC, gasket and sample crystal
DAC transmission min/max			0.91 / 1.00	0.92 / 1.00
Gasket shadowing min/max			0.69 / 0.95	0.72 / 0.95
Sample transmission min/max	T_{min} = 0.85 T_{max} = 0.85	T_{min} = 0.85 T_{max} = 0.85	0.85 / 0.86	0.85 / 0.87

[a] $w = 1/(\sigma^2(Fo^2)+x^2P^2+yP)$, where $P=(\mathrm{Max}(Fo^2, 0)+2Fc^2)/3$.

This journal is © The Royal Society of Chemistry 2012

Table S2. Atomic coordinates ($\cdot 10^4$), U_{eq} and U_{iso} ($Å^2 \cdot 10^3$) for C_2H_5Cl phase I at 120.0(1) and 100.0(1) K (all at 0.1 MPa) and phase II at 2.62(5) and 3.04(5) GPa (all at 295 K).

Atom	*x*/*a*	*y*/*b*	*z*/*c*	U_{eq}/U_{iso}
phase I at 120 K				
Cl1	2131(1)	9403(1)	8007(1)	51(1)
C1	−970(6)	8729(4)	7158(5)	49(1)
H11	−1036(105)	8590(46)	5849(85)	93(16)
H12	−1903(147)	9525(77)	7461(130)	147(33)
C2	−1508(7)	7491(4)	8223(6)	48(1)
H21	−3019(95)	7139(49)	7740(61)	63(12)
H22	−159(115)	6867(49)	7890(78)	92(15)
H23	−1418(92)	7639(39)	9561(84)	76(13)
phase I at 100 K				
Cl1	2164(1)	9404(1)	8063(1)	40(1)
C1	−951(5)	8722(4)	7152(5)	38(1)
H11	−903(80)	8561(38)	5794(69)	61(11)
H12	−2089(88)	9455(48)	7274(76)	68(16)
C2	−1500(6)	7489(3)	8268(5)	38(1)
H21	−2997(88)	7154(48)	7736(60)	54(11)
H22	−218(98)	6803(49)	8124(70)	73(12)
H23	−1470(60)	7657(31)	9625(55)	37(8)
phase II at 2.62 GPa				
Cl1	1091(1)	4544(1)	2500	32(1)
C1	−1216(4)	3049(4)	2500	30(1)
H1	−1622(29)	3336(27)	3772(31)	45(6)
C2	−1597(4)	1210(4)	2500	31(1)
H21	−2754(48)	473(46)	2500	47(9)
H22	−1113(31)	986(32)	1325(33)	55(6)
phase II at 3.04 GPa				
Cl1	1100(1)	4545(1)	2500	29(1)
C1	−1222(3)	3048(3)	2500	27(1)
H1	−1612(22)	3380(20)	3814(25)	38(5)
C2	−1614(4)	1190(3)	2500	28(1)
H21	−2770(39)	525(39)	2500	36(8)
H22	−1121(25)	978(28)	1243(28)	54(5)

This journal is © The Royal Society of Chemistry 2012

Table S3. Comparison of the interatomic distances and angles in the MCE phases I and II.

Phase I at:	**0.1 MPa/120 K**	**0.1 MPa/100 K**	**Phase II at:**	**2.62 GPa/295 K**	**3.04 GPa/295 K**
Cl1···Cl1^{i} (Å)	3.9642(16)	3.8737(14)	Cl1···Cl1^{p} (Å)	3.3657(13)	3.3263(11)
∠C1–Cl1···Cl1^{i} (º)	155.79(13)	157.73(11)	∠C1–Cl1···Cl1^{p} (º)	132.42(11)	132.02(10)
∠Cl1···Cl1^{i}–C1^{i} (º)	155.79(13)	157.73(11)	∠Cl1···Cl1^{p}–C1^{p} (º)	167.58(11)	167.98(10)
Cl1···Cl1^{j} (Å)	3.9593(14)	3.8915(13)	Cl1···Cl1^{q} (Å)	3.3657(13)	3.3263(11)
∠C1–Cl1···Cl1^{j} (º)	75.31(14)	75.40(11)	∠C1–Cl1···Cl1^{q} (º)	167.58(11)	167.98(10)
∠Cl1···Cl1^{j}–C1^{j} (º)	75.31(14)	75.40(11)	∠Cl1···Cl1^{q}–C1^{q} (º)	132.42(11)	132.02(10)
H22···Cl1^{k} (Å)	3.02(5)	3.03(5)	H1···Cl1^{r} (Å)	2.910(20)	2.840(16)
∠C2–H22···Cl1^{k} (º)	165(4)	167(4)	∠C1–H1···Cl1^{r} (º)	152.3(17)	154.1(13)
∠H22···Cl1^{k}–C1^{k} (º)	136.2(12)	133.9(10)	∠H1···Cl1^{r}–C1^{r} (º)	103.5(4)	103.2(3)
H12···Cl1^{l} (Å)	3.24(8)	3.16(5)	H1···Cl1^{r} (Å)	2.910(20)	2.840(16)
∠C1–H12···Cl1^{l} (º)	122(5)	130(3)	∠C1–H1···Cl1^{r} (º)	152.3(17)	154.1(13)
∠H12···Cl1^{l}–C1^{l} (º)	147.4(15)	143.3(9)	∠H1···Cl1^{r}–C1^{r} (º)	103.5(4)	103.2(3)
H23···Cl1^{m} (Å)	3.27(5)	3.24(3)	H21···Cl1^{s} (Å)	2.94(4)	2.90(3)
∠C2–H23···Cl1^{m} (º)	129(3)	129(3)	∠C2–H21···Cl1^{s} (º)	165(3)	170(3)
∠H23···Cl1^{m}–C1^{m} (º)	80.6(9)	78.9(6)	∠H21···Cl1^{s}–C1^{s} (º)	75.5(7)	74.1(6)
H21···H23^{n} (Å)	2.63(6)	2.60(6)	H22···H22^{t} (Å)	2.33(3)	2.24(3)
∠C2–H21···H23^{n} (º)	139(4)	142(3)	∠C2–H22···H22^{t} (º)	147.5(21)	147.1(17)
∠H21···H23^{n}–C2^{n} (º)	140(4)	136(3)	∠H22···H22^{t}–C2^{t} (º)	136.0(20)	135.0(17)
H23···H21^{o} (Å)	2.63(6)	2.60(6)	H22···H22^{u} (Å)	2.33(3)	2.24(3)
∠C2–H23···H21^{o} (º)	140(4)	136(3)	∠C2–H22···H22^{u} (º)	136.0(20)	135.0(17)
∠H23···H21^{o}–C2^{o} (º)	139(4)	142(3)	∠H22···H22^{u}–C2^{u} (º)	147.5(21)	147.1(17)

Symmetry codes: (^{i}) 1–*x*, 2–*y*, 2–*z*; (^{j}) –*x*, 2–*y*, 2–*z*; (^{k}) 0.5–*x*, –0.5+*y*, 1.5–*z*; (^{l}) –1+*x*, *y*, *z*; (^{m}) –0.5+*x*, 1.5–*y*, 0.5+*z*; (^{n}) –0.5+*x*, 1.5–*y*, –0.5+*z*; (^{o}) 0.5+*x*, 1.5–*y*, 0.5+*z*; (^{p}) –*x*+*y*, 1–*x*, *z*; (^{q}) 1–*y*, 1+*x*–*y*, *z*; (^{r}) –*x*, 1–*y*, 0.5+*z*; (^{s}) –1–*x*+*y*, –*x*, *z*; (^{t}) *y*, –*x*+*y*, –*z*; (^{u}) *x*–*y*, *x*, –*z*.